OPEN

Automated high-throughput heartbeat quantification in medaka and zebrafish embryos under physiological conditions

Jakob Gierten[1,2*], Christian Pylatiuk[3], Omar T. Hammouda[2], Christian Schock[3], Johannes Stegmaier[4], Joachim Wittbrodt[2], Jochen Gehrig[5*] & Felix Loosli[6*]

Accurate quantification of heartbeats in fish models is an important readout to study cardiovascular biology, disease states and pharmacology. However, dependence on anaesthesia, laborious sample orientation or requirement for fluorescent reporters have hampered the use of high-throughput heartbeat analysis. To overcome these limitations, we established an efficient screening assay employing automated label-free heart rate determination of randomly oriented, non-anesthetized medaka (*Oryzias latipes*) and zebrafish (*Danio rerio*) embryos in microtiter plates. Automatically acquired bright-field data feeds into an easy-to-use *HeartBeat* software with graphical user interface for automated quantification of heart rate and rhythm. Sensitivity of the assay was demonstrated by profiling heart rates during entire embryonic development. Our analysis revealed rapid adaption of heart rates to temperature changes, which has implications for standardization of experimental layout. The assay allows scoring of multiple embryos per well enabling a throughput of >500 embryos per 96-well plate. In a proof of principle screen for compound testing, we captured concentration-dependent effects of nifedipine and terfenadine over time. Our novel assay permits large-scale applications ranging from phenotypic screening, interrogation of gene functions to cardiovascular drug development.

Quantification of heartbeats is an important readout to study physiology and disease states of the heart. The resting heart rate (beats per minute, bpm) is a strong predictive risk factor of overall mortality and associated with a growing catalogue of genetic variants and environmental-sensitive alleles[1,2]. However, geneticists are facing an enormous challenge to establish causality for associated candidate variants. Small fish models provide efficient means of functional assessment in the context of a vertebrate. In fish models heart rate and rhythm quantification is employed for analysing inherited or acquired arrhythmia[3], for validation of genetic variants[4], phenotypic drug discovery and safety pipelines[5] or for toxicological studies[6]. Moreover, the recent establishment of a vertebrate panel of isogenic strains in medaka fish enables to study variations of quantitative traits such as heart rate in genome-wide association studies[7]. However, there is a lack of efficient screening workflows that allow large-scale quantitative scoring of cardiac phenotypes. Therefore, novel and efficient protocols were needed encompassing sample preparation, automated imaging and image analysis.

The fish species medaka (*Oryzias latipes*) and zebrafish (*Danio rerio*) emerged as major vertebrate models for phenotypic screening, follow-up functional studies, reverse genetics and for studying human pathologies in mechanistic details[8,9]. Medaka and zebrafish have tractable diploid genomes, feature a short generation time (2–3 months), external embryonic development and established protocols for transgenesis and manipulation of gene function including CRISPR/Cas-based approaches[10,11]. Economic husbandry and small transparent embryos are particularly suited for large-scale screening and detailed imaging[12,13]. In both fish species, rapid cardiovascular

[1]Department of Pediatric Cardiology, University Hospital Heidelberg, Heidelberg, Germany. [2]Centre for Organismal Studies, Heidelberg University, Heidelberg, Germany. [3]Institute for Automation and Applied Informatics, Karlsruhe Institute of Technology, Eggenstein-Leopoldshafen, Germany. [4]Institute of Imaging and Computer Vision, RWTH Aachen University, Aachen, Germany. [5]ACQUIFER is a division of DITABIS, Digital Biomedical Imaging Systems AG, Pforzheim, Germany. [6]Institute of Biological and Chemical Systems, Biological Information Processing (IBCS-BIP), Karlsruhe Institute of Technology, Eggenstein-Leopoldshafen, Germany. *email: jakob.gierten@med.uni-heidelberg.de; j.gehrig@acquifer.de; felix.loosli@kit.edu

development leads to a functional cardiovascular system emerging by around 24 hours post fertilization (hpf) in zebrafish[14] and approximately 48 hpf in medaka[15]. Although the fish heart is two-chambered, its development and function are very similar to the mammalian heart[16]. Strikingly, components of the electrocardiogram of zebrafish and medaka have more similarities to those in humans than have those of rodents, making them ideal models to investigate heart rate and rhythm phenotypes and leverage these properties for drug screens[17–19]. In contrast to mammalian models, early zebrafish embryos are sufficiently supplied by oxygen diffusion allowing the study of severe cardiovascular and dysfunctional haemoglobin phenotypes that result in embryonic lethality in mammals[20].

Readouts of heart rate and rhythm have been employed increasingly in zebrafish- and medaka-based screens[21–28]. Challenges of current methods to capture heart rate in high-throughput include: (i) immobilisation of dechorionated embryos or hatchlings, which in the majority of cases is achieved by anaesthesia with tricaine leading to severe adverse cardiovascular effects[29], (ii) imaging of larvae in standardized orientations, involving labour-intensive manual mounting on dedicated sample carriers or embedding in low-melting agarose, (iii) fluorescent reporter readouts, which preclude studies of specific genetic backgrounds and (iv) lack of user-friendly software for efficient analysis of multiple hearts simultaneously.

We therefore developed a high-throughput screening pipeline with simple sample handling and fully automated imaging of unhatched medaka and zebrafish embryos. Label-free imaging can be performed under physiological conditions and controlled temperature without anaesthesia or agarose-based mounting, and with scalable numbers of embryos per plate. The screening workflow is complemented by a user-friendly open-access software package, named *HeartBeat*, for robust quantification of heart rate and rhythm. Applied to both zebrafish and medaka we quantified native heart rate throughout development from heartbeat onset to hatching stage. To facilitate high-throughput applications, microplates containing up to 6 embryos per well were scored with high success rates and reliability. Additionally, we studied cardiac activity responses to temperature ramps enabling the analysis of physical stress response or profiling temperature-sensitive mutants. As a proof of concept for pharmacological screens, we tested nifedipine and terfenadine resulting in heart rate inhibition. This demonstrates the applicability to preclinical drug screens and toxicological tests using fish models.

Results

High-throughput assay and *HeartBeat* software.
We implemented a rapid workflow for automated imaging of medaka and zebrafish embryos and a new *HeartBeat* software for extraction of heart rate and rhythm. The multi-step pipeline is schematically summarized in Fig. 1. The transparent chorion naturally constrains embryonic movement and therefore supersedes anaesthesia or immobilisation. This allows simple sample preparation and high-throughput cardiac imaging in a physiological environment. Different speed of embryonic development of both fish species can be leveraged for heartbeat time-lapse imaging with different interval lengths ranging between ~24–72 hpf in zebrafish and ~2–7 dpf in medaka (Fig. 1a). Single or multiple unhatched embryos were analysed without requirements for positioning, orientation or special mounting medium. We used 96 well-plates as default but also other formats are compatible with the *HeartBeat* software. U-bottom plates are recommended for single embryos per well and F-bottom shapes for multiple embryos per well. A crucial feature of the imaging setup is a stationary plate holder combined with moving optics that eliminate plate movement artefacts and thus obviating mounting media with high viscosity (Fig. 1b). Processing with *HeartBeat* is compatible with a wide range of sampling rates, resolutions and illumination modes. Here, default settings for heart rate scoring were 13 fps with 2x detection objective (whole-well detection) and bright-field (Fig. 1b). For exact assessment of beat-to-beat variability, higher frame rates are recommended (see *HeartBeat* software).

Whole embryo image sequences are processed by three consecutive operations: (i) segmentation based on cumulative grey value differences in the input image sequence, smoothing and thresholding, (ii) feature extraction by calculating the standard deviation (s.d.) in identified segments over time, (iii) spectral analysis and classification of heart regions. Dialogue windows ask to specify a range of image sequences in a parent directory and the numbers of embryos contained in each well. Different numbers of fish to be analysed can be defined for multi-mounted wells. In a graphical user interface (GUI), processed time sequences and segments of classified heart regions (blue area) and s.d. traces are presented (Fig. 2a,c) and central settings can be navigated (Fig. 2b). Thus, visualization of segmentation and classified heartbeats over time allow for rapid quality check and adjustments. For each image sequence, detailed result files are saved as spreadsheets as well as a graphical overview of the segmentation (Fig. 2c). Heartrates of all wells are saved in one summary spreadsheet together with a heatmap in the corresponding parent directory of the dataset. In a sample of *myl7::eGFP* embryos acquired both in eGFP and BF channels, HR was scoreable in 100% in the GFP channel and 98.9% in bright-field (n = 92 embryos, data not shown). Heart rate scores inferred from both channels were highly correlated (Pearson correlation coefficient $r = 0.98$ for manual count vs. software readout in BF and $r = 0.95$ for software readout in GFP vs. software readout in BF; Supplementary Fig. S1). In summary, automated heart rate measurements on whole embryo BF images equally perform compared to readout of fluorescently labelled hearts.

Heartbeat detection of multiple embryos per well.
Upscaling the number of embryos per plate can significantly increase throughput for large-scale applications as more specimen can be assayed in a single microplate-wide recording. One option used in some whole-organism screening assays are 384 well plates, that would likewise be compatible with the analytical workflow presented in this study. However, parallel capturing of multiple embryos in a single image, additionally reduces the demand for data storage as well as time of imaging and analysis. For increased throughput, simultaneous readout of multiple fish hearts per imaging field was implemented in the *HeartBeat* algorithm. To assess conditions and efficiency of parallel readout in single wells, an experimental series of 1–6 and 10 embryos per well of 96-well plates were performed for medaka and zebrafish (Fig. 3a,b, respectively). Full-size image frames were used to analyse multiple embryos with random well positions to achieve correct scoring. Pairwise comparisons of the mean heart rate of mounting groups with
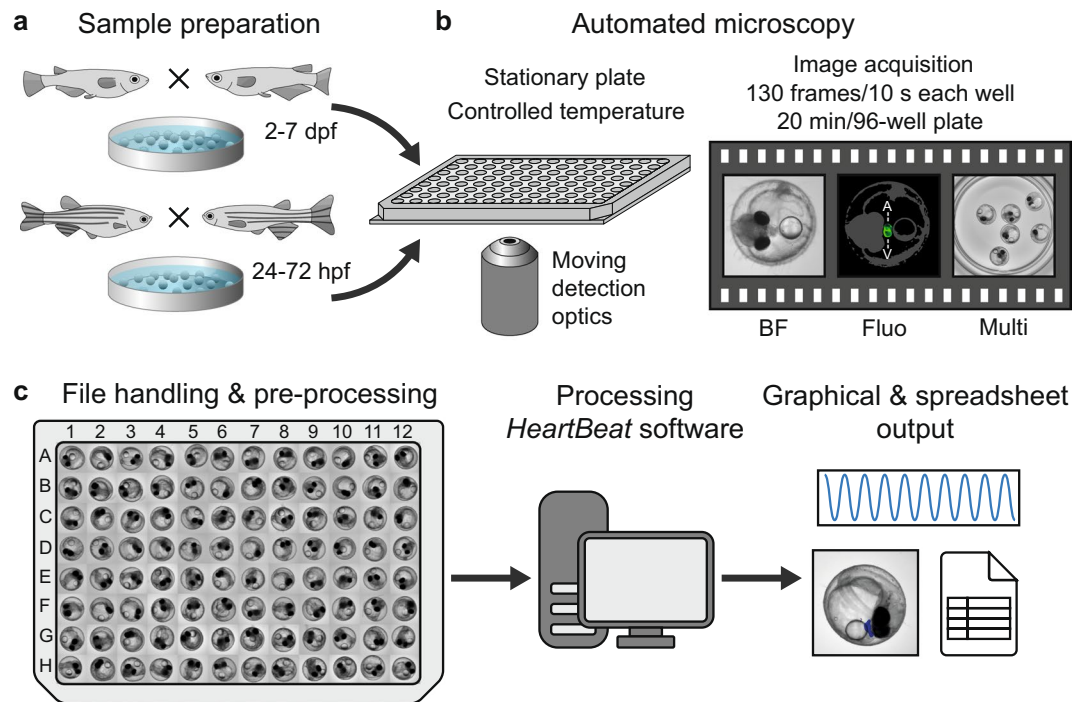
Figure 1. Workflow of automated imaging and heart rate quantification in medaka and zebrafish embryos. (**a**) Cardiovascular development is functional after 24 and 48 hpf and hatching occurs around 48–72 hpf and 7–8 dpf in zebrafish and medaka, accordingly, defining time windows of embryonic cardiac imaging in both fish species. (**b**) Single or multiple fish embryos per well are mounted without anaesthesia or agarose into microtiter plates, which have a fixed position in the imaging platform; image sequences can be sampled at different frame rates, resolutions and channels; all images were recorded with 2x objective, images with single embryos were cropped, multiple embryos in a well (Multi) are presented as full frame; in the fluorescent image A and V denote atrium and ventricle and a rough outline of the embryo is overlaid as a reference. (**c**) After image optimization, image sequences are quantified through a GUI of the *HeartBeat* program (compare Fig. 2) and heart rates, beat-to-beat variability and an overview of segmentation are saved as spreadsheet and graphical output, respectively.

≥2 embryos per well to the reference of 1 embryo per well, yielded for medaka a statistically significant elevation of heart rates in mounts with 2–6 embryos per well and a formally not significant difference for 10 embryos per well. However, increasing variance and numbers of outliers were observed in wells containing 10 embryos. The equivalent zebrafish experiment (Fig. 3b) revealed a higher baseline variability, whereas comparisons to the 1 embryo per well group did not reach statistical significance. A replicate of the experiment for medaka and zebrafish revealed similar results (data not shown). Different offsets of heart rates depending on the number of embryos per well can be controlled by using the same numbers of embryos per well for the entire plate. However, as 10 embryos per well could be scored less effective and yielded an increased number of outliers, a maximum through-put of 6 embryos per well is most efficient and stable. Taken together, the heart rate workflow presented here can be scaled up to 6 embryos per well. For comparability, all wells should be filled with the same number of embryos.

Heart rate dynamics in medaka and zebrafish development. We applied the assay to score heart rates during the entire development of medaka and zebrafish embryos. Onset of heartbeat varied in the two fish species with earliest heartbeats appearing after 22 hpf in zebrafish and 40 hpf in medaka. From this time points onwards, image data was captured every 4 h (Fig. 4). In medaka, embryonic heart rate was rapidly increasing over developmental time and started to oscillate in a day-night rhythm from 72 hpf onwards and reached approximately 175 bpm (at 28 °C) around hatching stage (7 dpf, Fig. 4a). Similarly, after onset of heartbeat in zebrafish, heart rate increased and plateaued at around 210 bpm (28 °C, 72 hpf; Fig. 4b). Zebrafish heart rate did not exhibit a day-night dependent fluctuation during the period of analysis (22–62 hpf).

Temperature-dependent modulation of heart rate. Ambient temperature is a critical environmental factor affecting heart rate in most teleosts. To quantify this effect, we studied the influence of ambient temperature changes on heart rate between 26–30 °C (Fig. 5). Heart rates, both in medaka and zebrafish, accelerated significantly per 1 °C increase of temperature. This finding underlines the importance of tight temperature control when assessing any heart-beat related cardiac phenotypes. The influence of the sampling rate on the assay sensitivity was further tested. Medaka and zebrafish heart rate quantification on a 30 fps data set and derived synthetic 15 fps data yielded comparable results (Supplementary Fig. S3). Moreover, an extended temperature range (21–35 °C) was measured, revealing anticipated prominent increases of embryonic heart rates in medaka and zebrafish, which could be used as a simple assay to study the mechanisms of genotype × environment interactions (Supplementary Fig. S4).
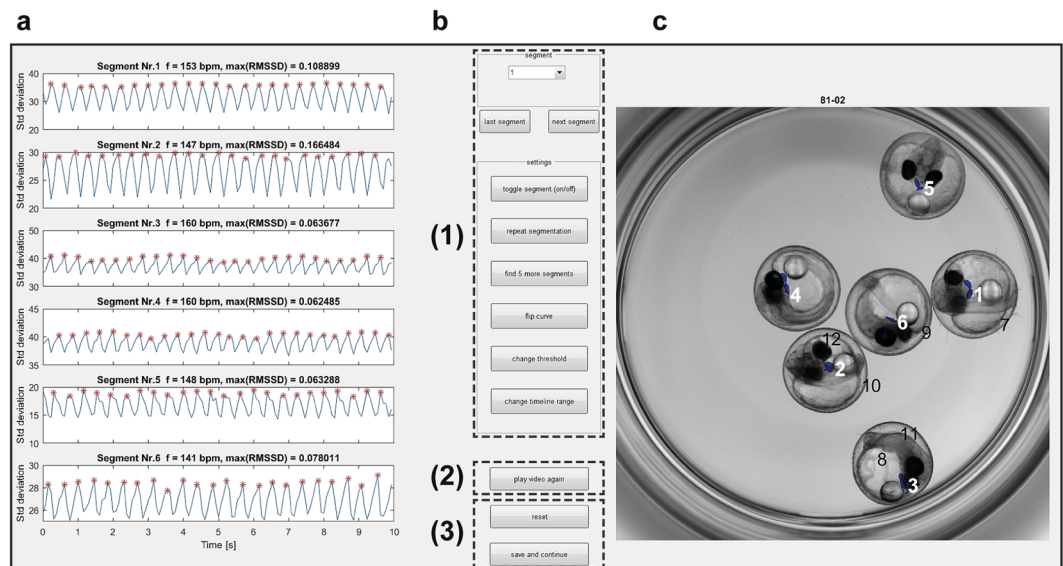
Figure 2. Functionalities of *HeartBeat* software. (**a**–**c**) Graphical user interface of the *HeartBeat* software for computer-assisted semi-automated analysis allowing convenient and rapid quality check. (**a**) Standard deviations of pixel values relating to segmented heart regions are displayed over time in the left panel, where heartbeats are indicated by red asterisks for each image sequence. (**b**) A control panel allows (1) to refine settings of segmentation and to choose alternative segments, (2) to re-play the current image sequence (visualized in **c**), (3) to reset all settings or to save heart rates to spreadsheets together with a picture of segmented image sequence. (**c**) Visualization of the image sequence with segmented heart regions displayed as numbered blue areas (detailed manual available together with software in Supplementary material online).
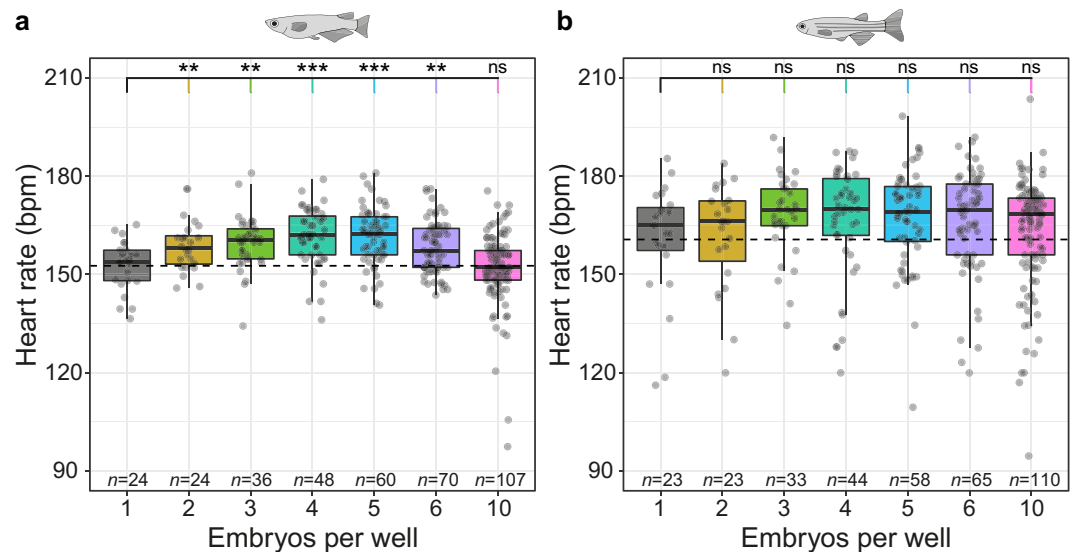

Figure 3. Heartbeat detection of multiple embryos per well. (**a**,**b**) Scoring of heart rate with 1–6 and 10 embryos per well for medaka at 102 hpf (**a**) and zebrafish at 34 hpf (**b**). Data is provided as box plots and scatter plots of original heart rate measurements. Heart rates of mounting groups with ≥ 2 embryos per well were each tested with Student's t-test against 1 embryo per well (dashed line indicates mean heart rate of the group with 1 embryo per well); significant differences are indicated with $*P < 0.05$, $**P < 0.01$ and $***P < 0.001$, ns (not significant); n for each group is indicated in the figure.

Compound effects on heart rate of unhatched medaka and zebrafish embryos.

Heart rate is frequently scored in preclinical screening assays of chemical compounds employing small fish models. To demonstrate the compatibility of our platform with high-throughput chemical screening, we trialled two pharmaceuticals, nifedipine and terfenadine, with known inhibitory effects on heart rate in fish[5,30]. In one 96-well plate, groups of 12 embryos were exposed to terfenadine and nifedipine each at 10, 30 and 100 µM. An internal plate control was kept in embryo medium (EMR/E3). After a baseline measurement, embryos were incubated in the
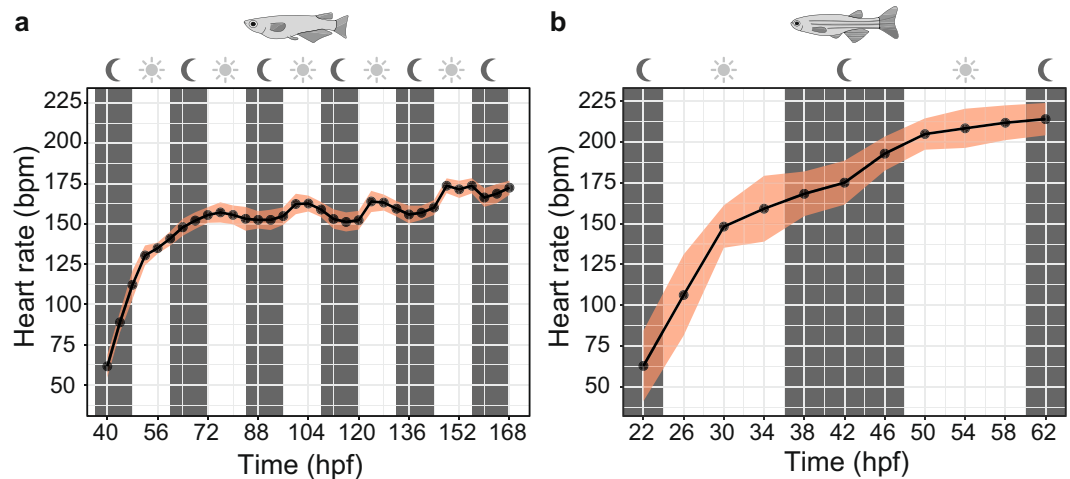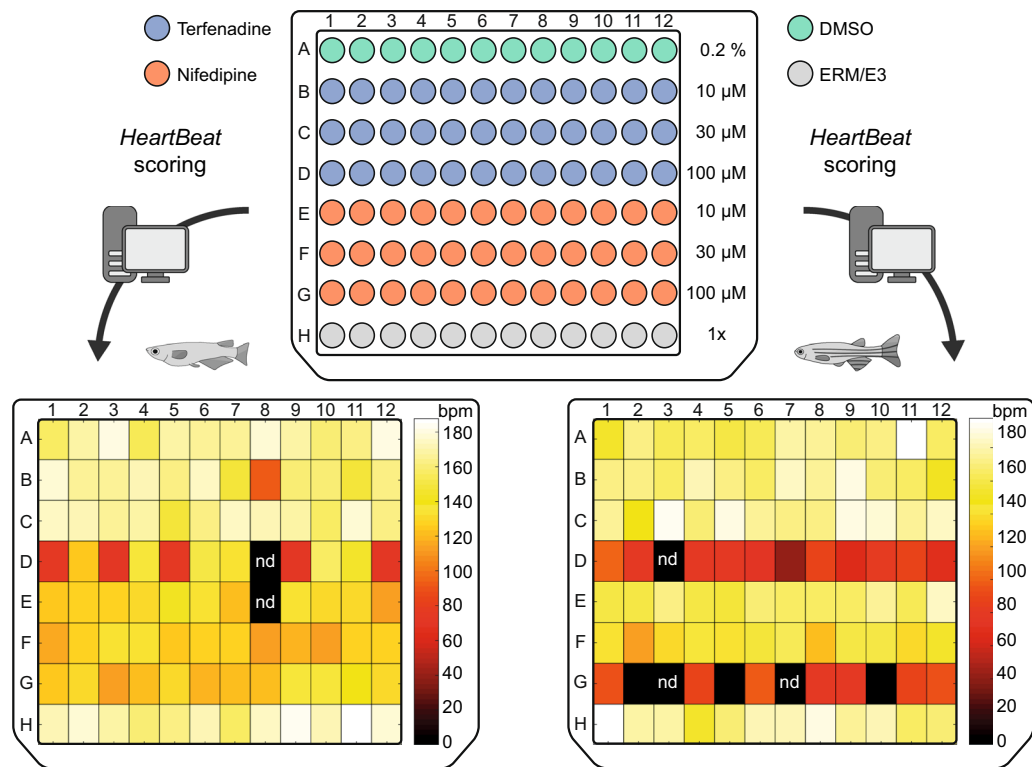
Figure 4. Heart rates of medaka and zebrafish during embryonic development. (**a,b**) Heart rates of unhatched embryos were measured from onset of heartbeat until hatching (details in Methods). (**a**) Circadian oscillation of heart rate in medaka from 3 dpf onwards (mean ± s.d., $n = 13$–18 each point in time). (**b**) In zebrafish, the onset of the heartbeat was followed by an immediate increase of heart rate passing into a less steep slope of increase at around 210 bpm (mean ± s.d., $n = 12$–52 each point in time).
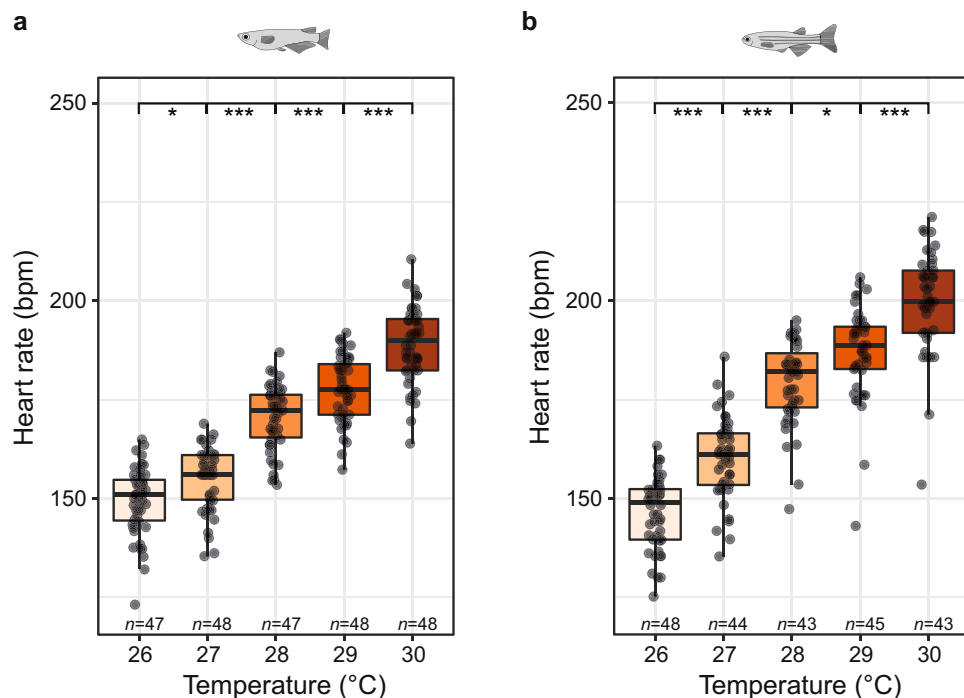
Figure 5. Temperature-dependent heart rate modulation. (**a,b**) Heart rate response to temperature gradients in medaka (100–102 hpf, $n = 47$–48 at each temperature in **a**) and zebrafish (31–33 hpf, $n = 43$–48 at each temperature in **b**) recorded at 13 fps. Significant differences between heart rates at each temperature were tested with one-way ANOVA and pairwise comparisons using Student's t-test and are given with $*P < 0.05$, $**P < 0.01$ and $***P < 0.001$ (significant differences are indicated only for 1 °C-increments; P-values for all pairs of combinations in **a,b** are given in Supplementary Table S1 and S2, respectively); data is presented as box plots (median±interquartile range) and overlaid scatter plots of heart rate values.

test and vehicle control (0.2% DMSO) solutions for 2 h and captured in 30 min intervals. For each heart rate data set of one microtiter plate, the *HeartBeat* software generates heatmaps for immediate intuitive assessment of drug effects; examples are shown at 90 min drug incubation (Fig. 6). Terfenadine elicited significant inhibition of heart rate at 100 µM both in medaka and zebrafish although with different dynamics. In medaka, 100 µM terfenadine induced a significant reduction of heart rate after 60 min treatment, which became more pronounced over time (Fig. 7a). It induced 2:1 atrioventricular (AV) block in some medaka embryos at 90 min and increasingly after

Figure 6. Quantification of heart rates in fish embryos treated with compounds. 96-well format for incubation of medaka and zebrafish embryos with terfenadine and nifedipine each at three different concentrations in µM. As a control for stage-dependent changes of heart rate, all measurements (drugs and DMSO) were normalized to a negative control group of age-matched untreated embryos (row H). The *HeartBeat* software directly provides a heatmap output for intuitive assessment of drug effects (heart rate response shown at 90 min; nd: not detected).

120 min drug exposure (Supplementary Video S1). In zebrafish embryos, 100 µM terfenadine suppressed heart rate earlier (30 min) and more markedly after 2 h incubation with a transient 2:1 AV block between 30–60 min resulting in dual-chamber suppression at 90 min onwards (Fig. 7b, Supplementary Video S2). The *HeartBeat* software extracts either atrial or ventricular beating rate, which is equal in the regularly beating heart. The random orientation of the embryos primarily influences whether the heart rate is measured on the atrium or the ventricle. Although the current *HeartBeat* software version does not measure chamber-specific rates, the AV block of terfenadine-treated embryos is nevertheless reflected by atrial rates or ventricular rates (the latter is 50% reduced) clustering to the upper or lower quartiles of the box plots, respectively (Fig. 7a, 100 µM terfenadine at 90 min and 120 min for medaka; Fig. 7b, 100 µM terfenadine at 30 min and 60 min for zebrafish). Nifedipine inhibited heart rates in medaka embryos equally at 10, 30 and 100 µM with rapid onset (Fig. 7a). In zebrafish embryos, heart rates were decreased by nifedipine in a concentration- and time-dependent manner resulting in asystole for the majority of embryos treated with 100 µM nifedipine for 120 min (Fig. 7b). To provide a reference for embryonic applications using DMSO carrier, heart rates were assessed for a concentration range of 0.2–1%. In medaka, heart rates were not significantly affected by different DMSO concentrations within 2 h of incubation, whereas minor heart rate fluctuations occurred at lower DMSO concentrations in zebrafish (Supplementary Fig. S2). As a control for stage-dependent changes of heart rate, all measurements (drugs and DMSO) were normalized to a negative control group of age-matched untreated embryos (Fig. 7 and Supplementary Fig. S2).

Discussion

Heart rate is a key parameter in numerous small fish model applications including genetics and pharmacology and a reliable metric for environmental studies assessing cardiotoxic and adverse developmental effects of small molecules and pollutants. Here, we present a physiological assay and open-access HeartBeat software for rapid quantitative assessment of heart rate and rhythm of medaka and zebrafish embryos with high analytical power in terms of precision and throughput that permits large-scale phenotypic scoring. The commercial imaging system used in this study provides an ideal platform with out of the box fulfilment of the imaging requirements, such as tight temperature control and non-moving specimen, thus allowing a rapid and highly-efficient implementation of the methodology. However, the core method is compatible with many other imaging modalities, including more cost-effective open hardware solutions for automated imaging[31]. The performance of our pipeline allowed to capture concentration-dependent effects of cardiovascular active drugs with high temporal resolution.

Our assay overcomes laborious manual mounting and orientation of samples, motion artefacts, confounding effects of anaesthesia and dependency on fluorescent reporters. Fast and reliable quantification of heart rate
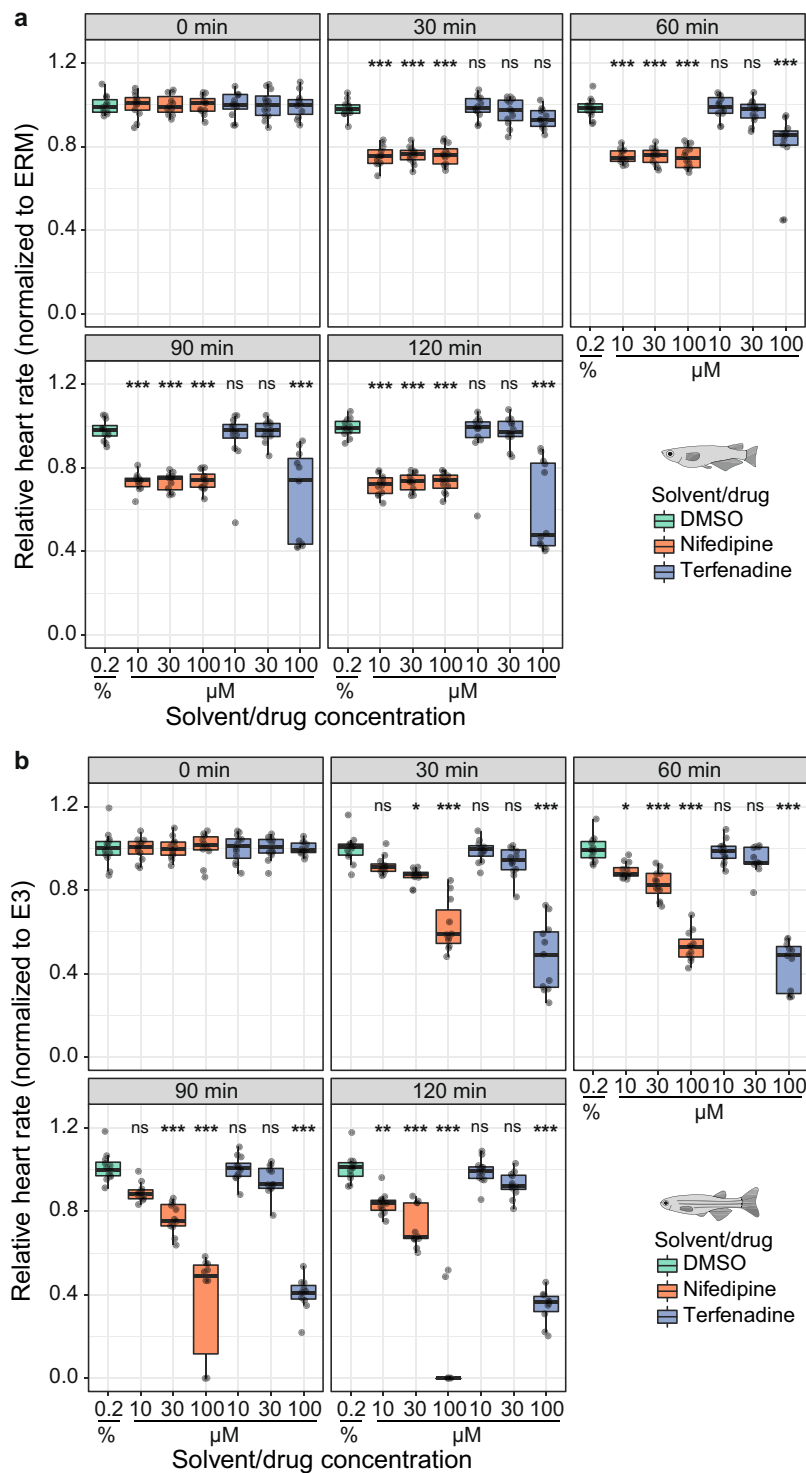
Figure 7. Heart rate inhibition by nifedipine and terfenadine over time. (**a**) Time course of drug effects revealing heart rate inhibition in medaka embryos (102–104 hpf) by nifedipine and 100 μM terfenadine ($n = 11$–12 each for DMSO, terfenadine 10/30/100 μM, nifedipine 10/30/100 μM at every time point). (**b**) Concentration-dependent heart rate decrease by nifedipine and terfenadine in zebrafish (32–34 hpf; $n = 10$–12 for all treatment and control groups at every time point). Significant difference between each drug concentration and the time-matched DMSO control group were tested with one-way ANOVA and pairwise comparisons using Student's t-test and are given with $*P < 0.05$, $**P < 0.01$ and $***P < 0.001$, ns (not significant); data is visualized as box plots (median ± interquartile range) and scatter plots of original data points. At all points in time, each heart rate measurement of one of the treatment groups is normalized to the mean heart rate of a control group in fish medium (ERM/medaka, E3/zebrafish; data not shown) to account for stage-dependent changes and is expressed relative to the corresponding baseline treatment group mean (time point 0).

is achieved by combining automated image acquisition of unhatched, randomly oriented fish embryos with software-based segmentation of heart regions and automatic heartbeat detection. Precise temperature control during automated imaging ensures reproducibility and cross-centre data comparability. The *HeartBeat* software was developed for user-independent, automatic segmentation of heart regions and feature extraction of rate and rhythmicity with high reliability and reproducibility. A GUI provides non-expert user swift computer-assisted analysis with control of key settings and visualization of analytic output. This interface minimizes user bias and permits to set standards for data comparability between experiments and research groups. A compiled version of the software can be executed with freely available MATLAB Runtime. Of note, heartbeat quantification can be performed robustly on bright-field image sequences with comparable efficiency to image sequences with labelled hearts. The analysis in bright-field mode is critical for rapid screening of multiple wild-type strains without fluorescent reporters. The software is compatible with many imaging setups with manual or automated recording using different magnifications. We chose a sampling rate of 13 Hz sufficient for frequencies of heartbeats in medaka and zebrafish embryos. Maximal heart rates at 35 °C were 278.6 bpm (4.62 Hz) and 325 bpm (5.42 Hz) in medaka and zebrafish, respectively (Fig. 5). At 28 °C, average heart rates were at 163 bpm (2.72 Hz, medaka) and 197 bpm (3.28 Hz, zebrafish; Fig. 5). For analysis of beat-to-beat intervals, however, we recommend sampling at higher frame rates. These frame rates are compatible with standard microscopy equipment. Together with the *HeartBeat* software we provide scripts for file parsing and image optimization, which can be adapted to individual setups and data handling. Cropping to single embryos increased performance, further improved scoring success by eliminating spurious background signals in a storage space efficient manner. TIFF and JPEG compressed image sequences are equally compatible with the *HeartBeat* software. The compatibility with compressed image data massively reduces data volumes, thus facilitating the data transfer across remote collaborators.

To explore the maximal throughput, *HeartBeat* software was applied to readout multiple fish per well and reliably captured heart rates of up to 10 embryos per well. Differences between mean heart rates extracted from wells with different embryo densities (Fig. 3) might be reflecting varying physiological environments. For comparative assays this needs to be controlled by using the same numbers of embryos per well for the entire plate. Automated capturing of multiple hearts was performed most efficiently up to 6 embryos per well resulting in >500 embryos processed per 96-well plate, particularly suitable for drug screening pipelines.

To date, several methods have been used to assess heartbeat in zebrafish hatchlings, medaka embryos, fish species, Drosophila, cardiomyocytes or mouse embryos[21,22,24,25,27,28,32–36]. Some of these methods require transgenic embryos with fluorescent cardiomyocytes or erythrocytes to measure heartbeats[26,32]. Other approaches depend on advanced microscopes such as confocal laser scanning microscope[26] or dual-beam optical reflectometer[34], imaging modalities that may affect sample temperature and confounding effects on heart rate (Fig. 5). Another caveat is immobilisation of fish larvae in low-melting agarose to achieve specific orientations, which is time-consuming and complicates genuine high-throughput assays. Some methods were restricted to a narrow time window of newly hatched zebrafish prior to swim bladder inflation to avoid movements of the larvae during sampling[28,32]. In addition, larvae were acclimatized to the illumination of the well scans. To achieve stable imaging condition many protocols rely on anesthesia[21,22,24,27,33]. The most widely used anaesthetic is tricaine (MS-222, ethyl 3-aminobenzoate methanesulfonate), that affects cardiovascular functions including heart rate and contractility[37,38]. Our assay, on the other hand, relies on recording non-anesthetized unhatched medaka and zebrafish embryos in their natural environment within the chorion allowing fast sample distribution into microtiter plate, and is compatible with robotic handling of fish embryos in systematic screens[39,40].

We demonstrate robust heart rate quantification of randomly positioned and oriented fish embryos and implemented options in the *HeartBeat* GUI to easily improve the accuracy of heartbeat detection, such as changing the threshold of detection, if necessary. Full 96-well plates are imaged in 20 min with 10 s videos at 13 fps for each well. High-confidence quantification can be performed within 45–60 min. In the meantime, our reliable and efficient assay permitted us to automatically quantify heart rate of more than 20 000 image sequences corresponding to approximately 20 TB of data.

While only scant data of embryonic medaka heart rate was available[15], using the *HeartBeat* assay we now provide a systematic profile as reference for future studies (Fig. 4a). Interestingly, after 3 days of development heart rate in medaka showed day-night undulation with a nocturnal dipping resembling the circadian heart rate patterns in healthy humans[41]. Zebrafish has faster embryogenesis and morphological differentiation including looping of the heart is completed by 36 hpf[42]. Serial recordings from onset of heartbeat onwards reliably delineated the rapid increase of heart rate associated with major steps of cardiac development within the first 2.5 dpf (Fig. 4b). As aerobic capacity and metabolic rate are directly interrelated with ambient temperature, incremental warming (Fig. 5 and Supplementary Fig. S4) can be applied as physical stressor in ectothermic medaka and zebrafish embryos, which regulate cardiac output in response to temperature primarily through adaption of heart rate rather than stroke volume[43,44]. Tight control of heart rate by temperature can be leveraged as readout of acute and chronic adaptive stress responses, temperature-sensitive strains[45] and of susceptibility to arrhythmia in strains with different genetic backgrounds. In summary, our detailed analysis stresses the importance to rigorously control temperature and normalize to stage-dependent changes of beat rates to ensure experimental standardization.

Medaka and zebrafish embryos are mostly transparent around the heart region, providing ideal conditions for direct microscopic observation of the beating heart. Heart rate is a suitable metric to efficiently assess therapeutic and adverse actions of drugs as demonstrated by previous reports using zebrafish hatchlings[32]. To assess the applicability of our assay based on non-hatched embryos for compound treatment and to benchmark the analysis software, we designed proof-of-concept experiments using nifedipine and terfenadine. Concentration-dependent heart rate inhibition and dynamic changes of drug effects were recorded in a 2 h time-lapse experiment, reliably correlating with published negative chronotropic effects of terfenadine and nifedipine in zebrafish[5,30]. In human, the antihistamine terfenadine can induce adverse prolongation of QT interval resulting in increased risk for torsades de pointes tachycardia. Detailed studies have demonstrated QT prolongation resulting in AV block in

zebrafish[46] and medaka[45]. Probing effects of terfenadine on zebrafish and medaka embryonic heart rate, distinct time points of induction and time courses of AV block were uncovered by our assay (Fig. 7). In zebrafish, nifedipine suppresses cardiac Ca^{2+} channels resulting in a marked decrease of heart rate[30,47]. This drug action was reliably monitored with our assay showing significant effects ranging from sustained inhibition to asystole over time (Fig. 7). However, for genuine screening in drug discovery applications, substance-specific effective concentrations and bioavailability need to be considered for the experimental design and precisely controlled under particular technical conditions. Taken together, this proof of concept pharmacological experiment in combination with the scalability of our assay raises the prospect of accelerating drug discovery pipelines and rapid pre-clinical prediction of adverse drug effects.

In summary, by combining ease and stability of imaging acquisition with software-assisted analysis our method offers a comprehensive platform for forward and reverse genetics, gene x environment interaction studies, pharmaceutical screens and toxicological assessment, which can efficiently direct downstream studies on mechanistical details of heart rate related phenotypes.

Methods

Fish husbandry and transgenic line.
The inbred, isogenic medaka strain Cab and wild type zebrafish AB were kept in closed stocks at the Institute of Biological and Chemical Systems, Biological Information Processing (IBCS-BIP) at the Karlsruhe Institute of Technology (KIT) and the Centre for Organismal Studies (COS) at Heidelberg University as previously described[48,49]. Fish husbandry was performed in accordance with EU directive 2010/63/EU guidelines as well as with German animal protection regulations (Tierschutzgesetz §11, Abs. 1, no. 1; Regierungspräsidium Karlsruhe, Germany; husbandry permits AZ35-9185.64/BH KIT and AZ35-9185.64/BH Wittbrodt). The fish facilities are under the supervision of the Regierungspräsidium Karlsruhe, who approved the experimental procedures. Embryos were raised at 28 °C. Embryonic stages are indicated in hours post fertilization (hpf) or days post fertilization (dpf)[15,50].

For fluorescent cardiac imaging in medaka, a transgenic line *myl7::eGFP* was generated. A modified plasmid pDestTol2CG (http://tol2kit.genetics.utah.edu/index.php/PDestTol2CG) containing a *myl7::eGFP* cassette was co-injected with Tol2 transposase mRNA into Cab embryos as described[51].

Sample preparation and time-lapse experiments.
One day prior to imaging medaka eggs were optically cleared by rolling the eggs on sandpaper (P1000). One hour before imaging, medaka and zebrafish embryos were transferred from methylene blue-containing medium into plain ERM and E3, respectively. Single medaka/zebrafish embryos were mounted with 150 µl ERM/E3 per well in transparent round (U) bottom 96-well plates (Thermo Fisher Scientific, 268152) using Cell-Saver tips (Biozym). Multi-mounts ($\geq$ 2 embryos/well) were prepared with 300 µl ERM/E3 per well using flat (F) bottom 96-well plates (Greiner, 655101).

For time-lapse heart rate measurements microtiter plates were kept between 08:00–20:00 in the incubator at 28 °C and transferred to the microscope with 15 min equilibration time before acquiring two loops at 12:00 and 16:00. During night cycle the plate remained in the microscope (constant 28 °C) and 4 loops were recorded with 4 h intervals between 20:00–08:00. For all other experiments, medaka embryos were imaged at day 4 post fertilization (start of recordings at 100–104 hpf) and zebrafish embryos at 1.5 days post fertilization (start of recordings at 32–36 hpf) as indicated for each experiment.

Solutions and drug administration.
Terfenadine and nifedipine (Sigma, Steinheim, Germany) were prepared as 50 mM stock solutions in dimethylsulphoxide (DMSO) and stored at −20 °C. Prior to application, stock solutions were diluted in ERM (medaka) or E3 (zebrafish) to the desired final concentrations; light-sensitive nifedipine was prepared freshly for each experiment. DMSO (vehicle control) and drug incubation experiments were performed with single mounted embryos. For each plate a baseline was recorded in ERM/E3 at 28 °C (see automated microscopy) followed by exchange of the medium with test substances. Prior to the first loop of imaging during drug incubation, embryos were allowed to equilibrate in the incubation chamber of the microscope for min. 15 min to max. 30 min after drug transfer to the plate (equals first point in time).

Automated microscopy.
96-well microtiter plates containing zebrafish or medaka embryos were sealed with gas-permeable adhesive foil (4titude, Wotton, UK, 4ti-0516/96). After equilibration for 15 min in the incubation chamber of the microscope under bright-field illumination, the plates were automatically imaged on an ACQUIFER Imaging Machine, a wide-field high content screening microscope equipped with a white LED array for bright-field imaging, a LED fluorescence excitation light source, a sCMOS (2048 × 2048 pixel) camera, a stationary plate holder, movable optics and a temperature-controlled incubation lid (DITABIS AG, Pforzheim, Germany). The focal plane was detected in the bright-field channel using a software autofocus algorithm. Images were acquired using 130 z-slices (dz = 0 µm) with a 2× Plan UW N.A. 0.06 (Nikon, Düsseldorf, Germany) leading to the acquisition of a 10 s movie with 13 fps at the very same z-axis position that is determined by the built-in software autofocus. Integration times were fixed with 80% relative LED intensity in bright-field and 100% in GFP-channel with 10 ms exposure time, generating image sequences of entire microwells of approximately 10 s with 13 fps. Capturing an entire 96-well plate generates 12480 frames resulting in 97.5 GB for full camera sensor readout size. Each microtiter plate was imaged once at 26 °C, 27 °C, 28 °C, 29 °C, and 30 °C or with the indicated time-lapse in case of drug exposures.

HeartBeat detection and analysis software.
Image optimization was performed prior to the heart rate analysis (Supplementary material online). Based on previous expertise[25], a new *HeartBeat* software was developed in MATLAB (Mathworks) for embryonic heart rate quantification and segmentation of multiple hearts in a field

of view. The *HeartBeat* software features a graphical user interface (GUI) for direct application by non-expert users (detailed instructions for operation see Supplementary material online). It is executable with MATLAB runtime (MATLAB 2017) on a Windows computer and available through https://osf.io/kygd4/. We recommend sufficient main memory ($\geq$16 GB RAM) and a solid-state disk hard drive or other storage solution with high I/O rates.

Data analysis and statistics.   Statistical analyses were computed in R language[52] and data visualized using the ggplot2 package[53]. Differences between samples were tested with Student's *t*-test and statistical significance accepted at a threshold of $P < 0.05$. Multiple comparisons were tested with one-way ANOVA and significant results ($P < 0.05$) were analysed with pairwise comparisons using Student's *t*-test applying significance levels adjusted with the Bonferroni method. Significant *P*-values are indicated with asterisks (*) with *$P < 0.05$, **$P < 0.01$ and ***$P < 0.001$. Correlation analysis was performed using Pearson's correlation.

Data and Code availability

The *HeartBeat* analysis software and supporting scripts are available through https://osf.io/kygd4/ in open access. Datasets supporting the findings of this study will be provided as spreadsheets by the corresponding authors upon request.

References

1. Hoed den, M. *et al*. Identification of heart rate-associated loci and their effects on cardiac conduction and rhythm disorders. *Nat. Genet.* **45**, 621–631 (2013).
2. Eppinga, R. N. *et al*. Identification of genomic loci associated with resting heart rate and shared genetic predictors with all-cause mortality. *Nat. Genet.* **48**, 1557–1563 (2016).
3. Hassel, D. *et al*. Deficient zebrafish ether-a-go-go-related gene channel gating causes short-QT syndrome in zebrafish reggae mutants. *Circulation* **117**, 866–875 (2008).
4. Ma, J.-F. *et al*. TBX5 mutations contribute to early-onset atrial fibrillation in Chinese and Caucasians. *Cardiovasc. Res.* **109**, 442–450 (2016).
5. Milan, D. J., Peterson, T. A., Ruskin, J. N., Peterson, R. T. & MacRae, C. A. Drugs that induce repolarization abnormalities cause bradycardia in zebrafish. *Circulation* **107**, 1355–1358 (2003).
6. Singh, A. P. *et al*. Ponatinib-induced cardiotoxicity: delineating the signaling mechanisms and potential rescue strategies. *Cardiovasc. Res.* **67**, 7 (2019).
7. Spivakov, M. *et al*. Genomic and phenotypic characterization of a wild medaka population: towards the establishment of an isogenic population genetic resource in fish. *G3* **4**, 433–445 (2014).
8. Lieschke, G. J. & Currie, P. D. Animal models of human disease: zebrafish swim into view. *Nat. Rev. Genet.* **8**, 353–367 (2007).
9. Kirchmaier, S., Naruse, K., Wittbrodt, J. & Loosli, F. The genomic and genetic toolbox of the teleost medaka (Oryzias latipes). *Genet.* **199**, 905–918 (2015).
10. Shah, A. N., Davey, C. F., Whitebirch, A. C., Miller, A. C. & Moens, C. B. Rapid reverse genetic screening using CRISPR in zebrafish. *Nat. Methods* **12**, 535–540 (2015).
11. Stemmer, M., Thumberger, T., Del Sol Keyer, M., Wittbrodt, J. & Mateo, J. L. CCTop: An Intuitive, Flexible and Reliable CRISPR/Cas9 Target Prediction Tool. *PLoS ONE* **10**, e0124633 (2015).
12. Lischik, C. Q., Adelmann, L. & Wittbrodt, J. Enhanced *in vivo*-imaging in medaka by optimized anaesthesia, fluorescent protein selection and removal of pigmentation. *PLoS ONE* **14**, e0212956 (2019).
13. Wagner, N. *et al*. Instantaneous isotropic volumetric imaging of fast biological processes. *Nat. Methods* **16**, 497–500 (2019).
14. Stainier, D. Y. & Fishman, M. C. The zebrafish as a model system to study cardiovascular development. *Trends Cardiovasc. Med.* **4**, 207–212 (1994).
15. Iwamatsu, T. Stages of normal development in the medaka Oryzias latipes. *Mech. Dev.* **121**, 605–618 (2004).
16. Gut, P., Reischauer, S., Stainier, D. Y. R. & Arnaout, R. Little Fish, Big Data: Zebrafish As A Model For Cardiovascular And Metabolic Disease. *Physiol. Rev.* **97**, 889–938 (2017).
17. Arnaout, R. *et al*. Zebrafish model for human long QT syndrome. *Proc. Natl. Acad. Sci. USA* **104**, 11316–11321 (2007).
18. MacRae, C. A. & Peterson, R. T. Zebrafish as tools for drug discovery. *Nat. Rev. Drug. Discov.* **14**, 721–731 (2015).
19. Yonekura, M. *et al*. Medaka as a model for ECG analysis and the effect of verapamil. *J. Pharmacol. Sci.* **137**, 55–60 (2018).
20. Warren, K. S. & Fishman, M. C. 'Physiological genomics': mutant screens in zebrafish. *Am. J. Physiol.* **275**, H1–7 (1998).
21. Chan, P. K., Lin, C. C. & Cheng, S. H. Noninvasive technique for measurement of heartbeat regularity in zebrafish (Danio rerio) embryos. *BMC Biotechnol.* **9**, 11 (2009).
22. Fink, M. *et al*. A new method for detection and quantification of heartbeat parameters in Drosophila, zebrafish, and embryonic mouse hearts. *Biotechniques* **46**, 101–113 (2009).
23. Spomer, W., Pfriem, A., Alshut, R., Just, S. & Pylatiuk, C. High-throughput screening of zebrafish embryos using automated heart detection and imaging. *J. Lab. Autom.* **17**, 435–442 (2012).
24. Yozzo, K. L., Isales, G. M., Raftery, T. D. & Volz, D. C. High-content screening assay for identification of chemicals impacting cardiovascular function in zebrafish embryos. *Env. Sci. Technol.* **47**, 11302–11310 (2013).
25. Pylatiuk, C. *et al*. Automatic zebrafish heartbeat detection and analysis for zebrafish embryos. *Zebrafish* **11**, 379–383 (2014).
26. De Luca, E. *et al*. ZebraBeat: a flexible platform for the analysis of the cardiac rate in zebrafish embryos. *Sci. Rep.* **4**, 835–13 (2014).
27. Puybareau, E., Genest, D., Barbeau, E., Léonard, M. & Talbot, H. An automated assay for the assessment of cardiac arrest in fish embryo. *Comput. Biol. Med.* **81**, 32–44 (2017).
28. Martin, W. K. *et al*. High-Throughput Video Processing of Heart Rate Responses in Multiple Wild-type Embryonic Zebrafish per Imaging Field. *Sci. Rep.* **9**, 145 (2019).
29. Huang, W.-C. *et al*. Combined use of MS-222 (tricaine) and isoflurane extends anesthesia time and minimizes cardiac rhythm side effects in adult zebrafish. *Zebrafish* **7**, 297–304 (2010).
30. Langheinrich, U., Vacun, G. & Wagner, T. Zebrafish embryos express an orthologue of HERG and are sensitive toward a range of QT-prolonging drugs inducing severe arrhythmia. *Toxicol. Appl. Pharmacol.* **193**, 370–382 (2003).
31. Pylatiuk, C., Vogt, M., Scheikl, P. & Gottwald, A. E. Automated Versatile DIY Microscope Platform. *Conf. Proc. IEEE Eng. Med. Biol. Soc.* **2018**, 5310–5312 (2018).

32. Burns, C. G. *et al*. High-throughput assay for small molecules that modulate zebrafish embryonic heart rate. *Nat. Chem. Biol.* **1**, 263–264 (2005).
33. Taylor, J. M., Girkin, J. M. & Love, G. D. High-resolution 3D optical microscopy inside the beating zebrafish heart using prospective optical gating. *Biomed. Opt. Express* **3**, 3043–3053 (2012).
34. Lai, Y.-C., Chang, W.-T., Lin, K.-Y. & Liau, I. Optical assessment of the cardiac rhythm of contracting cardiomyocytes *in vitro* and a pulsating heart *in vivo* for pharmacological screening. *Biomed. Opt. Express* **5**, 1616–1625 (2014).
35. Nepstad, R., Davies, E., Altin, D., Nordtug, T. & Hansen, B. H. Automatic determination of heart rates from microscopy videos of early life stages of fish. *J. Toxicol. Environ. Health Part. A* **80**, 932–940 (2017).
36. Sala, L. *et al*. MUSCLEMOTION: A Versatile Open Software Tool to Quantify Cardiomyocyte and Cardiac Muscle Contraction *In Vitro* and *In Vivo*. *Circ. Res.* **122**, e5–e16 (2018).
37. Craig, M. P., Gilday, S. D. & Hove, J. R. Dose-dependent effects of chemical immobilization on the heart rate of embryonic zebrafish. *Lab. Anim.* **35**, 41–47 (2006).
38. Haverinen, J., Hassinen, M., Korajoki, H. & Vornanen, M. Cardiac voltage-gated sodium channel expression and electrophysiological characterization of the sodium current in the zebrafish (Danio rerio) ventricle. *Prog. Biophys. Mol. Biol.* **138**, 59–68 (2018).
39. Pfriem, A. *et al*. A modular, low-cost robot for zebrafish handling. *Conf. Proc. IEEE Eng. Med. Biol. Soc.* **2012**, 980–983 (2012).
40. Graf, S. F., Hötzel, S., Liebel, U., Stemmer, A. & Knapp, H. F. Image-based fluidic sorting system for automated Zebrafish egg sorting into multiwell plates. *J. Lab. Autom.* **16**, 105–111 (2011).
41. Degaute, J. P., van de Borne, P., Linkowski, P. & Van Cauter, E. Quantitative analysis of the 24-hour blood pressure and heart rate patterns in young men. *Hypertension* **18**, 199–210 (1991).
42. Stainier, D. Y., Lee, R. K. & Fishman, M. C. Cardiovascular development in the zebrafish. I. Myocardial fate map and heart tube formation. *Dev.* **119**, 31–40 (1993).
43. Little, A. G. & Seebacher, F. Thyroid hormone regulates cardiac performance during cold acclimation in zebrafish (Danio rerio). *J. Exp. Biol.* **217**, 718–725 (2014).
44. Lee, L. *et al*. Functional Assessment of Cardiac Responses of Adult Zebrafish (Danio rerio) to Acute and Chronic Temperature Change Using High-Resolution Echocardiography. *PLoS ONE* **11**, e0145163 (2016).
45. Watanabe-Asaka, T. *et al*. Regular heartbeat rhythm at the heartbeat initiation stage is essential for normal cardiogenesis at low temperature. *BMC Dev. Biol.* **14**, 12 (2014).
46. Jou, C. J. *et al*. An *in vivo* cardiac assay to determine the functional consequences of putative long QT syndrome mutations. *Circ. Res.* **112**, 826–830 (2013).
47. Nemtsas, P., Wettwer, E., Christ, T., Weidinger, G. & Ravens, U. Adult zebrafish heart as a model for human heart? An electrophysiological study. *J. Mol. Cell. Cardiol.* **48**, 161–171 (2010).
48. Loosli, F. *et al*. A genetic screen for mutations affecting embryonic development in medaka fish (Oryzias latipes). *Mech. Dev.* **97**, 133–139 (2000).
49. d'Alençon, C. A. *et al*. A high-throughput chemically induced inflammation assay in zebrafish. *BMC Biol.* **8**, 151 (2010).
50. Kimmel, C. B., Ballard, W. W., Kimmel, S. R., Ullmann, B. & Schilling, T. F. Stages of embryonic development of the zebrafish. *Dev. Dyn.* **203**, 253–310 (1995).
51. Thermes, V. *et al*. I-SceI meganuclease mediates highly efficient transgenesis in fish. *Mech. Dev.* **118**, 91–98 (2002).
52. R Core Team. R: A Language and Environment for Statistical Computing, Available at, https://www.R-project.org/ (2016).
53. Wickham, H. ggplot2: elegant graphics for data analysis. (Springer-Verlag, 2009).

Acknowledgements

Author contributions

Ja.G., Jo.G. and F.L. designed the study and implemented the methodology. C.P., C.S., J.S., Jo.G. and Ja.G. developed software. Ja.G. generated the transgenic line. Ja.G., O.T.H. and Jo.G. performed experiments. Ja.G., C.P. and O.T.H. analysed data. Ja.G., C.P. and Jo.G. conducted data validation. Ja.G. visualized data. Ja.G., Jo.G., C.P., F.L. and J.W. wrote the manuscript. F.L., J.W. and Jo.G. provided resources. J.W., F.L. and C.P. supervised this work.

Competing interests

Jochen Gehrig is an employee of DITABIS AG, Pforzheim, Germany. All other authors declare no competing interests.

Additional information

Supplementary information is available for this paper at https://doi.org/10.1038/s41598-020-58563-w.

Correspondence and requests for materials should be addressed to J. Gierten or J. Gehrig or F.L.

Reprints and permissions information is available at www.nature.com/reprints.

Publisher's note Springer Nature remains neutral with regard to jurisdictional claims in published maps and institutional affiliations.